

# Isospin-Violating Dark Matter in the $U(1)'$ Model Inspired by $E_6$

Tianjun Li,<sup>1,2,3,\*</sup> Qian-Fei Xiang,<sup>4,†</sup> Qi-Shu Yan,<sup>3,‡</sup> Xianhui Zhang,<sup>3,§</sup> and Han Zhou<sup>2,3,¶</sup>

<sup>1</sup>*Institute of Theoretical Physics, Jiangxi Normal University, Nanchang 330022, P. R. China*

<sup>2</sup>*CAS Key Laboratory of Theoretical Physics and Kavli Institute for Theoretical Physics China (KITPC), Institute of Theoretical Physics, Chinese Academy of Sciences, Beijing 100190, P. R. China*

<sup>3</sup>*School of Physical Sciences, University of Chinese Academy of Sciences, No. 19A Yuquan Road, Beijing 100049, P. R. China*

<sup>4</sup>*Center for High-Energy Physics, Peking University, Beijing, 100871, P. R. China*

(Dated: February 17, 2020)

## Abstract

We propose a  $U(1)'$  model inspired by  $E_6$  which has an isospin-violation dark matter. With extra two pairs of vector-like quarks, we can assign the proper  $U(1)'$  charges for the first two-generation quark doublets, and explain why the first two-generation quarks are lighter than the third generation. By choosing a proper linear combination of two extra  $U(1)$  gauge symmetries in  $E_6$ , it is natural to realize the ratio  $f_n/f_p = -0.7$  so as to maximally relax the constraints from the Xenon based direct detection experiments. We study the sensitivities of the dark matter direct and indirect detection experiments, and identify the parameter spaces that can give the observed relic density. We also study the sensitivities of the future colliders with center mass energy  $\sqrt{s}=33/50/100$  TeV, and compare the different detection methods. We show that in some parameter spaces the future colliders can give much stronger limits.

PACS numbers: 12.10.-g, 12.60.-i, 95.35.+d

---

\* tli@itp.ac.cn

† xiangqf@pku.edu.cn

‡ yanqishu@ucas.ac.cn

§ zhangxianhui16@mails.ucas.ac.cn

¶ zhouhan@itp.ac.cn

## I. INTRODUCTION

The observations of astrophysics and cosmology reveal that the main component of matter in the Universe is Dark Matter (DM). However, till now, all evidence for DM is through its gravitational effects, and the nature of DM particles remains a mystery. Determining the fundamental nature of the dark matter particle is one of the most important problems in particle and astro-particle physics. Great efforts have been taken to identify dark matter, including direct detection, indirect detection, and collider searches, while the answer is still unclear.

DM would be detectable through their elastic scattering with nuclei in terrestrial particle detectors. The most remarkable DM signals is the one claimed by the DAMA Collaboration (including DAMA/NaI and DAMA/LIBRA experiment) [1–5], which uses a NaI-based scintillation detector. With data collected over 14 annual cycles, the statistical significance of DAMA/LIBRA-phase2 has reached  $12.9\sigma$  [5]. The CoGeNT experiment, using Germanium as a target, also found an irreducible excess [6] and annual modulation [7]. The low energy excesses in the  $\text{CaWO}_4$  based experiment CRESST-II have been reported as well [8]. However, these observations are challenged by the null results of the other experiments, such as PandaX-II (2017) [9], LUX (2017) [10], and XENON1T (2018) [11].

The Isospin-Violating Dark Matter (IVDM), in which DM couples differently to protons and neutrons, has been proposed to reconcile the tensions among the different direct detection experimental results [12]. Recently, the COSINE-100 experiment, that also uses the same NaI crystal as target, observes no signal excess in the first 59.5 days of data [13]. This observation makes it difficult to explain all the direct detection observations, especially the observations of DAMA. In some particular models, such as the proton-philic spin-dependent inelastic Dark Matter (pSIDM), one could still explain DAMA modulation amplitude consistent with the constraints from other experiments [14]. Here we only focus on the concept of how to realize the isospin violation in a UV complete model, instead of trying to explain all experimental observations.

Nowadays the most stringent constraint on the DM-nucleus scattering cross sections is from the Xenon based experiments [9–11]. In this work, we will maximally relax these constraints by naturally realizing [12]

$$\frac{f_n}{f_p} \simeq -0.7 . \quad (1)$$

Several IVDM models have been proposed in recent years. For scalar dark matter, Ref. [15] proposed a model with colored mediators and Ref. [16] considered a two-Higgs doublet model. For Dirac dark matter, an effective  $Z'$  model was proposed in Ref. [17], a double portal scenario was considered in Ref. [18], and a string-theory inspired UV model was studied

in [19]. Within the framework of supersymmetry, different realizations were examined [20–22]. In this work, we propose a  $U(1)'$  Model with  $E_6$  origin.  $E_6$  is of particular interesting in the sense that it is anomaly free, and its fundamental representation is chiral representation. In particular, the  $U(1)'$  gauge anomaly cancellations in our models are inspired from  $E_6$ .

It is well-known that in the  $U(1)'$  models with  $E_6$  origin, the vector coupling of the up-type quarks to the  $Z'$  boson should be zero while their axial coupling may have non-zero value. Thus, one cannot realize the isospin-violation with  $f_n/f_p \simeq -0.7$  in the  $U(1)'$  model from  $E_6$ . To solve this problem, we introduce extra two pairs of vector-like quarks, and assign proper  $U(1)'$  charges for the first two-generation quark doublets. Interestingly, we can explain why the first two-generation quarks are lighter than the third generation as well. Considering a proper linear combination of two extra  $U(1)$  gauge symmetries in  $E_6$ , we naturally realize  $f_n/f_p = -0.7$  in the  $E_6$  inspired  $U(1)'$  model. We consider the constraints from dark matter direct and indirect detection experiments, and find that there are parameter spaces in our model which can give the correct DM relic density. Furthermore, we compare the sensitivities of the DM direct/indirect detection experiments and the future colliders with center mass energy  $\sqrt{s} = 33/50/100$  TeV. It is shown that in some parameter spaces the future colliders can provide much stronger limits.

The layout of this paper is as follows. In Sec. II, we describe the  $E_6$ -inspired  $U(1)'$  model. In Sec. III, we present constraints of dark matter direct detection experiments considering isospin violation effects. Sec. IV give the expected sensitivity of future proton-proton colliders on our model. Finally, we conclude in Sec. V.

## II. $E_6$ INSPIRED $U(1)'$ MODEL WITH ISOSPIN-VIOLATING DARK MATTER

We propose the  $U(1)'$  model with IVDM, which is a special subgroup of the  $E_6$  Grand Unified Theory (GUT) [23–33]. Its fundamental representation decomposes under  $SO(10)$  as

$$\mathbf{27} = \mathbf{16} + \mathbf{10} + \mathbf{1} .$$

The representation  $\mathbf{16}$  contains the 15 SM fermions, as well as a right-handed neutrino. It decomposes under  $SU(5)$  as

$$\mathbf{16} = \mathbf{10} + \bar{\mathbf{5}} + \mathbf{1} .$$

The  $\mathbf{10}$  representation under  $SU(5)$  decomposes as

$$\mathbf{10} = \mathbf{5} + \bar{\mathbf{5}} .$$

$SO(10)$	$SU(5)$	$2\sqrt{10}Q_\chi$	$2\sqrt{6}Q_\psi$	$4\sqrt{181}Q'$
<b>16</b>	<b>10</b> ( $Q_i, U_i^c, E_i^c$ )	-1	1	-9
	<b><math>\bar{5}</math></b> ( $D_i^c, L_i$ )	3	1	25
	<b>1</b> ( $N_i^c/T$ )	-5	1	-43
<b>10</b>	<b>5</b> ( $XD_i, XL_i^c/H_u$ )	2	-2	18
	<b><math>\bar{5}</math></b> ( $XD_i^c, XL_i/H_d$ )	-2	-2	-16
<b>1</b>	<b>1</b> ( $XN_i/S$ )	0	4	-2

TABLE I: Decomposition of the  $E_6$  fundamental **27** representation under  $SO(10)$ ,  $SU(5)$ , and the  $U(1)_\chi$ ,  $U(1)_\psi$  and  $U(1)'$  charges of multiplets. The SM quark doublets, right-handed up-type quarks, right-handed down-type quarks, lepton doublets, right-handed charged leptons, and right-handed neutrinos are labeled as  $Q_i$ ,  $U_i^c$ ,  $D_i^c$ ,  $L_i$ ,  $E_i^c$ , and  $N_i^c$ , respectively.

The **5** contains a color triplet and a  $SU(2)_L$  doublet, whereas  $\bar{\mathbf{5}}$  contains a color anti-triplet and another  $SU(2)$  doublet, and the **1** is a SM singlet. The gauge boson is contained in the adjoint **78** representation of  $E_6$ . The particle content of the **27** representation, which contains the SM fermions as well as extra fermions, are shown in the first two columns of Table I. The SM has three generations of fermion, so we use three such **27**.

The  $E_6$  gauge symmetry can be broken as follows [34, 35]

$$E_6 \rightarrow SO(10) \times U(1)_\psi \rightarrow SU(5) \times U(1)_\chi \times U(1)_\psi . \quad (2)$$

The  $U(1)_\psi$  and  $U(1)_\chi$  charges for the  $E_6$  fundamental **27** representation are also given in Table I.

The  $U(1)'$  attracting us is one linear combination of the  $U(1)_\chi$  and  $U(1)_\psi$

$$Q' = \cos \theta Q_\chi + \sin \theta Q_\psi . \quad (3)$$

The other  $U(1)$  gauge symmetry from the orthogonal linear combination as well as the  $SU(5)$  is broken at a high scale. This allows us to have a large doublet-triplet splitting scale, which prevents rapid proton decay if the  $E_6$  Yukawa relations were enforced. This will need either two pairs of (**27**,  $\bar{\mathbf{27}}$ ) or one pair of (**27**,  $\bar{\mathbf{27}}$ ), **78**, in addition to one pair of (**351'**,  $\bar{\mathbf{351'}}$ ) dimensional Higgs representations (Detailed studies of  $E_6$  theories with broken Yukawa relations can be found in [36, 37].) For our model, the unbroken symmetry at the TeV scale is  $SU(3)_C \times SU(2)_L \times U(1)_Y \times U(1)'$ .

In our model we introduce three fermionic **27**s, two pairs of vector-like fermions, one scalar Higgs doublet field  $H_u$  from the doublet of **5** of  $SU(5)$ , one scalar Higgs doublet field

$H_d$  from the doublet of  $\bar{\mathbf{5}}$  of  $SU(5)$ , one scalar SM singlet Higgs field  $T$  from the singlet of  $\mathbf{16}$  of  $SO(10)$ , and one scalar SM singlet Higgs field  $S$  from the singlet of  $\mathbf{27}$  of  $E_6$ . In particular, to realize the isospin violation, we assume that the first two generations of the left-handed quark doublets  $Q_k$  have  $U(1)'$  charge 9, while  $Q_3$  and  $XQ_k$  have  $U(1)'$  charge  $-9$ , where  $k = 1, 2$ . To cancel the gauge anomalies, we introduce  $\overline{XQ}_k$ . Note that the additional fermions from the  $\mathbf{27}$  with masses at the TeV scale are  $N_i^c$ ,  $XD_i$ ,  $XL_i^c$ ,  $XD_i^c$ ,  $XQ_k$ ,  $\overline{XQ}_k$ ,  $XL_i$ , and  $XN_i$ . For details, please see Table II.

By choosing

$$\tan \theta = -\frac{1}{17}\sqrt{3/5}, \quad (4)$$

it is natural to realize IVDM with  $f_n/f_p = -0.7$ .

$Q_k$	$(\mathbf{3}, \mathbf{2}, \mathbf{1/6}, \mathbf{9})$	$Q_3/XQ_k$	$(\mathbf{3}, \mathbf{2}, \mathbf{1/6}, -\mathbf{9})$	$\overline{XQ}_k$	$(\bar{\mathbf{3}}, \mathbf{2}, -\mathbf{1/6}, -\mathbf{9})$
$U_i^c$	$(\bar{\mathbf{3}}, \mathbf{1}, -\mathbf{2/3}, -\mathbf{9})$	$D_i^c$	$(\bar{\mathbf{3}}, \mathbf{1}, \mathbf{1/3}, \mathbf{25})$	$L_i$	$(\mathbf{1}, \mathbf{2}, -\mathbf{1/2}, \mathbf{25})$
$E_i^c$	$(\mathbf{1}, \mathbf{1}, \mathbf{1}, -\mathbf{9})$	$N_i^c/T$	$(\mathbf{1}, \mathbf{1}, \mathbf{0}, -\mathbf{43})$	$XD_i$	$(\mathbf{3}, \mathbf{1}, -\mathbf{1/3}, \mathbf{18})$
$XL_i^c, H_u$	$(\mathbf{1}, \mathbf{2}, \mathbf{1/2}, \mathbf{18})$	$XD_i^c$	$(\bar{\mathbf{3}}, \mathbf{1}, \mathbf{1/3}, -\mathbf{16})$	$XL_i, H_d$	$(\mathbf{1}, \mathbf{2}, -\mathbf{1/2}, -\mathbf{16})$
$XN_i, S$	$(\mathbf{1}, \mathbf{1}, \mathbf{0}, -\mathbf{2})$	$\chi$	$(\mathbf{1}, \mathbf{1}, \mathbf{0}, -\mathbf{27/2})$	$\Phi$	$(\mathbf{1}, \mathbf{1}, \mathbf{0}, \mathbf{86})$
$S'$	$(\mathbf{1}, \mathbf{1}, \mathbf{0}, \mathbf{18})$	$\phi$	$(\mathbf{1}, \mathbf{1}, \mathbf{0}, \mathbf{4})$	$\Phi'$	$(\mathbf{1}, \mathbf{1}, \mathbf{0}, \mathbf{1})$
$\phi'$	$(\mathbf{1}, \mathbf{1}, \mathbf{0}, \mathbf{7})$	$\phi''$	$(\mathbf{1}, \mathbf{1}, \mathbf{0}, \mathbf{5})$		

TABLE II: The quantum number assignment for particles under  $SU(3)_C \times SU(2)_L \times U(1)_Y \times U(1)'$  gauge symmetry,  $i = 1, 2, 3$ , and  $k = 1, 2$ . Here, the correct  $U(1)'$  charges are the  $U(1)'$  charges in the Table divided by  $4\sqrt{181}$ .

Three SM singlet Higgs fields  $\Phi$ ,  $\phi$ , and  $S'$  with  $U(1)'$  charges  $\mathbf{86}$ ,  $\mathbf{4}$ , and  $\mathbf{18}$  are introduced to generate the masses for  $N_i^c$ ,  $XN_i$ , and vector-like fermions  $(XQ_k, \overline{XQ}_k)$ , respectively. In order to break the global symmetries in the Higgs potential and avoid the massless Nambu-Goldstone bosons, we introduce two SM singlet Higgs fields  $\Phi'$ ,  $\phi'$ , and  $\phi''$  with  $U(1)'$  charges  $\mathbf{1}$ ,  $\mathbf{7}$ , and  $\mathbf{5}$ , respectively. Moreover, to introduce a dark matter candidate, we introduce a SM singlet Dirac fermion  $\chi$  with  $U(1)'$  charge  $-\mathbf{27/2}$ , which will not affect the gauge anomaly cancellations. In particular, only the  $U(1)'$  charge of  $\chi$  is a half integer while the  $U(1)'$  charges of all the other particles are integers. And then after  $U(1)'$  gauge symmetry breaking, there exists a residual discrete  $Z_2$  gauge symmetry under which  $\chi$  is odd while all the other particles are even. Thus,  $\chi$  cannot decay and can be a dark matter candidate. For details, please see Table II as well.

The interesting question is whether  $\chi$ ,  $(Q_K, \overline{XQ}_k)$ ,  $\Phi$ ,  $S'$ ,  $\phi$ ,  $\Phi'$ ,  $\phi'$ , and  $\phi''$  can arise from the higher representations of  $E_6$  since they do not belong to the fundamental  $\mathbf{27}$  representation of  $E_6$ . And let us discuss it one by one.

First,  $\chi$  cannot arise from the  $E_6$  representations since it is stable and cannot decay due to the discrete  $Z_2$  gauge symmetry from  $U(1)'$  gauge symmetry breaking. Also,  $\chi$  is a Dirac fermion and then might play a role of asymmetric dark matter which can affect the calculation of the dark matter relic density. This is very interesting, but for simplicity, we shall not consider it here.

Second, to address whether  $(Q_K, \overline{XQ_k})$  can arise from the higher representations of  $E_6$ , we only need to consider  $Q_k$  for simplicity. We can list all the particles from the higher representations of  $E_6$  whose quantum numbers under  $SU(3)_C \times SU(2)_L \times U(1)_Y \times U(1)'$  are  $(\mathbf{3}, \mathbf{2}, 1/6, \mathbf{Q}')$  as follows

$$\begin{aligned}
(\mathbf{3}, \mathbf{2}, 1/6, -54) &\subset \mathbf{2925} \text{ of } E_6, \\
(\mathbf{3}, \mathbf{2}, 1/6, -52) &\subset \overline{\mathbf{351}'} \text{ of } E_6, \\
(\mathbf{3}, \mathbf{2}, 1/6, -50) &\subset \mathbf{351}, \text{ and } \mathbf{1728} \text{ of } E_6, \\
(\mathbf{3}, \mathbf{2}, 1/6, -48) &\subset \mathbf{2430}, \text{ and } \mathbf{2925} \text{ of } E_6, \\
(\mathbf{3}, \mathbf{2}, 1/6, -11) &\subset \overline{\mathbf{351}'}, \text{ and } \overline{\mathbf{1728}} \text{ of } E_6, \\
(\mathbf{3}, \mathbf{2}, 1/6, -10) &\subset \mathbf{650} \text{ of } E_6, \\
(\mathbf{3}, \mathbf{2}, 1/6, -9) &\subset \mathbf{27}, \mathbf{351}, \mathbf{351}', \text{ and } \mathbf{1728} \text{ of } E_6, \\
(\mathbf{3}, \mathbf{2}, 1/6, -7) &\subset \mathbf{78}, \mathbf{650}, \mathbf{2430}, \text{ and } \mathbf{2925} \text{ of } E_6, \\
(\mathbf{3}, \mathbf{2}, 1/6, 32) &\subset \mathbf{351}, \text{ and } \mathbf{1728} \text{ of } E_6, \\
(\mathbf{3}, \mathbf{2}, 1/6, 34) &\subset \mathbf{78}, \mathbf{650}, \mathbf{2430}, \text{ and } \mathbf{2925} \text{ of } E_6, \\
(\mathbf{3}, \mathbf{2}, 1/6, 75) &\subset \mathbf{2430}, \text{ and } \mathbf{2925} \text{ of } E_6, \\
(\mathbf{3}, \mathbf{2}, 1/6, 77) &\subset \overline{\mathbf{1728}} \text{ of } E_6.
\end{aligned} \tag{5}$$

Therefore,  $(Q_K, \overline{XQ_k})$  cannot arise from the higher representations of  $E_6$ .

Third, to address whether the scalars  $\Phi$ ,  $S'$ ,  $\phi$ ,  $\Phi'$ ,  $\phi'$ , and  $\phi''$  can arise from the higher representations of  $E_6$ , we present all the particles from the higher representations of  $E_6$

whose quantum numbers under  $SU(3)_C \times SU(2)_L \times U(1)_Y \times U(1)'$  are  $(\mathbf{1}, \mathbf{1}, \mathbf{0}, \mathbf{Q}')$  as follows

$$\begin{aligned}
(\mathbf{1}, \mathbf{1}, \mathbf{0}, -\mathbf{86}) &\subset \overline{\mathbf{351}'} \text{ of } E_6, \\
(\mathbf{1}, \mathbf{1}, \mathbf{0}, -\mathbf{84}) &\subset \mathbf{1728} \text{ of } E_6, \\
(\mathbf{1}, \mathbf{1}, \mathbf{0}, -\mathbf{82}) &\subset \mathbf{2430} \text{ of } E_6, \\
(\mathbf{1}, \mathbf{1}, \mathbf{0}, -\mathbf{45}) &\subset \overline{\mathbf{351}'} \text{ of } E_6, \\
(\mathbf{1}, \mathbf{1}, \mathbf{0}, -\mathbf{44}) &\subset \mathbf{650} \text{ of } E_6, \\
(\mathbf{1}, \mathbf{1}, \mathbf{0}, -\mathbf{43}) &\subset \mathbf{27}, \mathbf{351}, \text{ and } \mathbf{1728} \text{ of } E_6, \\
(\mathbf{1}, \mathbf{1}, \mathbf{0}, -\mathbf{41}) &\subset \mathbf{78}, \mathbf{2430}, \text{ and } \mathbf{2925} \text{ of } E_6, \\
(\mathbf{1}, \mathbf{1}, \mathbf{0}, -\mathbf{39}) &\subset \overline{\mathbf{1728}} \text{ of } E_6, \\
(\mathbf{1}, \mathbf{1}, \mathbf{0}, -\mathbf{4}) &\subset \overline{\mathbf{351}'} \text{ of } E_6, \\
(\mathbf{1}, \mathbf{1}, \mathbf{0}, -\mathbf{2}) &\subset \mathbf{27}, \mathbf{351}, \text{ and } \mathbf{1728} \text{ of } E_6.
\end{aligned} \tag{6}$$

The singlet scalar particles with positive charges can be obtained from above particles via Hermitian conjugate. Therefore,  $\Phi$  and  $\phi$  can arise from the  $\mathbf{351}'$  representation of  $E_6$ , while  $S'$ ,  $\Phi'$ ,  $\phi'$ , and  $\phi''$  cannot arise from the higher representations of  $E_6$ .

Interestingly,  $(Q_K, \overline{XQ_k})$ ,  $S'$ ,  $\Phi'$ ,  $\phi'$ , and  $\phi''$  might emerge as the composite states. For example,  $Q_K$  can arise from  $(\mathbf{78}/\mathbf{650}/\mathbf{2430}/\mathbf{2925} \times \mathbf{351}') \times \mathbf{351}' \times \mathbf{351}' \times \mathbf{351}'$ ,  $\overline{XQ_k}$  can arise from the Hermitian conjugates of the above terms,  $S'$  can arise from  $(\overline{\mathbf{27}}/\overline{\mathbf{351}}/\overline{\mathbf{1728}}) \times \mathbf{351}' \times \mathbf{351}' \times \mathbf{351}' \times \mathbf{351}'$ ,  $\Phi'$  can arise from  $\mathbf{351}' \times \mathbf{650}$  or  $\overline{\mathbf{650}} \times (\mathbf{27}/\mathbf{351}/\mathbf{1728})$ ,  $\phi'$  can arise from  $\mathbf{351}' \times \overline{\mathbf{650}} \times (\mathbf{78}/\mathbf{2430}/\mathbf{2925})$ , and  $\phi''$  can arise from  $\overline{\mathbf{650}} \times \overline{\mathbf{1728}}$ .

The Higgs potential for the  $U(1)'$  gauge symmetry breaking is

$$\begin{aligned}
V = & -m_S^2|S|^2 - m_T^2|T|^2 - m_\Phi^2|\Phi|^2 - m_{S'}^2|S'|^2 - m_\phi^2|\phi|^2 - m_{\phi'}^2|\phi'|^2 - m_{\Phi'}^2|\Phi'|^2 - m_{\phi''}^2|\phi''|^2 \\
& + \lambda_S|S|^4 + \lambda_T|T|^4 + \lambda_\Phi|\Phi|^4 + \lambda_{S'}|S'|^4 + \lambda_\phi|\phi|^4 + \lambda_{\phi'}|\phi'|^4 + \lambda_{\Phi'}|\Phi'|^4 + \lambda_{\phi''}|\phi''|^4 \\
& + \lambda_{ST}|S|^2|T|^2 + \lambda_{S\Phi}|S|^2|\Phi|^2 + \lambda_{SS'}|S|^2|S'|^2 + \lambda_{S\phi}|S|^2|\phi|^2 + \lambda_{S\phi'}|S|^2|\phi'|^2 + \lambda_{S\Phi'}|S|^2|\Phi'|^2 \\
& + \lambda_{S\phi''}|S|^2|\phi''|^2 + \lambda_{T\Phi}|T|^2|\Phi|^2 + \lambda_{TS'}|T|^2|S'|^2 + \lambda_{T\phi}|T|^2|\phi|^2 + \lambda_{T\phi'}|T|^2|\phi'|^2 + \lambda_{T\Phi'}|T|^2|\Phi'|^2 \\
& + \lambda_{T\phi''}|T|^2|\phi''|^2 + \lambda_{\Phi S'}|\Phi|^2|S'|^2 + \lambda_{\Phi\phi}|\Phi|^2|\phi|^2 + \lambda_{\Phi\phi'}|\Phi|^2|\phi'|^2 + \lambda_{\Phi\Phi'}|\Phi|^2|\Phi'|^2 + \lambda_{\Phi\phi''}|\Phi|^2|\phi''|^2 \\
& + \lambda_{S'\phi}|S'|^2|\phi|^2 + \lambda_{S'\phi'}|S'|^2|\phi'|^2 + \lambda_{S'\Phi}|S'|^2|\Phi|^2 + \lambda_{S'\phi''}|S'|^2|\phi''|^2 + \lambda_{\phi\phi'}|\phi|^2|\phi'|^2 + \lambda_{\phi\Phi'}|\phi|^2|\Phi'|^2 \\
& + \lambda_{\phi\phi''}|\phi|^2|\phi''|^2 + \lambda_{\phi'\Phi'}|\phi'|^2|\Phi'|^2 + \lambda_{\phi'\phi''}|\phi'|^2|\phi''|^2 + \lambda_{\Phi'\phi''}|\Phi'|^2|\phi''|^2 \\
& + (A_1 S H_d H_u + A_2 T^2 \Phi + A_3 S(\Phi')^2 + A_4 S^2 \phi + A_5 S \phi'(\phi'')^\dagger + A_6 \phi \Phi'(\phi'')^\dagger \\
& + \lambda_1(\phi^2)^\dagger \phi' \Phi' + \lambda_2(S')^2 \phi' T + \lambda_3 \Phi'^2 (H_d H_u)^\dagger + \lambda_4 \phi'' S^2 (\Phi')^\dagger + \lambda_5(\phi')^\dagger \phi'' (\Phi')^2 \\
& + \lambda_6 \phi'(\phi'')^\dagger (H_d H_u)^\dagger + \lambda_7 S^\dagger (\phi')^2 \phi + \text{H.c.}) .
\end{aligned} \tag{7}$$

Note that without the  $A_i$  and  $\lambda_i$  terms in the bracket, there are ten global  $U(1)$  symmetries for the field  $S$ ,  $T$ ,  $\Phi$ ,  $S'$ ,  $\phi$ ,  $\Phi'$ ,  $\phi'$ ,  $\phi''$ ,  $H_u$ , and  $H_d$ . After they obtain the Vacuum Expectation

Values (VEVs), we have ten Goldstone bosons, where two of them are eaten by  $U(1)_Y$  and the extra  $U(1)'$  gauge boson. Thus, to avoid the extra Goldstone bosons, we need the  $A_i$  and  $\lambda_i$  terms to break eight global  $U(1)$  symmetries. By the way,  $\lambda_1$  term can be regarded as the combination of  $A_3$ ,  $A_4$ ,  $A_5$ , and  $A_6$  terms,  $\lambda_3$  term can be regarded as the combination of  $A_1$  and  $A_3$  terms,  $\lambda_4$  term can be regarded as the combination of  $A_4$  and  $A_6$  terms,  $\lambda_5$  term can be regarded as the combination of  $A_3$  and  $A_5$  terms, and  $\lambda_6$  term can be regarded as the combination of  $A_1$  and  $A_5$  terms. Thus, we are left with only two global symmetries in the above potential, which are  $U(1)_Y$  and the extra  $U(1)'$  gauge symmetry. Also,  $S$ ,  $T$ ,  $\Phi$ ,  $S'$ ,  $\phi$ ,  $\Phi'$ ,  $\phi'$ , and  $\phi''$  will mix with each other via the quartic and trilinear terms. In addition, the  $U(1)'$  symmetry breaking Higgs fields  $S$ ,  $T$ ,  $\Phi$ ,  $S'$ ,  $\phi$ ,  $\Phi'$ ,  $\phi'$ ,  $\phi''$  and the electroweak symmetry breaking Higgs fields  $H_u$  and  $H_d$  can be mixed via the quartic terms as well, for example,  $|S|^2|H_u|^2$ , etc, which can be written down easily. For simplicity, we will not study it here, and neglect the mass terms and quartic terms for  $H_u$  and  $H_d$  as well.

The Yukawa couplings in our models are

$$\begin{aligned}
-\mathcal{L} = & y_{3i}^U Q_3 U_i^c H_u + y_{ki}^U X Q_k U_i^c H_u + y_{3i}^D Q_3 D_i^c H_d + y_{ki}^D X Q_k D_i^c H_d + y_{k3}^{XQ} S' \overline{X Q_k} Q_3 \\
& + y_{kl}^{XQ} S' \overline{X Q_k} X Q_l + y_{ij}^E L_i E_j^c H_d + y_{ij}^N L_i N_j^c H_u + y_{ij}^{XNd} X L_i^c X N_j H_d \\
& + y_{ij}^{XNu} X L_i X N_j H_u + y_{ij}^{TD} D_i^c X D_j T + y_{ij}^{TL} X L_i^c L_j T + y_{ij}^{SD} X D_i^c X D_j S \\
& + y_{ij}^{SL} X L_i^c X L_j S + y_{ij}^{Nc} N_i^c N_j^c \Phi + y_{ij}^{XN} X N_i X N_j \phi + M_\chi^D \bar{\chi} \chi + M_{kl} \overline{X Q_k} Q_l + \text{H.c.} , \quad (8)
\end{aligned}$$

where  $i, j = 1, 2, 3$ , and  $k, l = 1, 2$ . Thus, after  $S$ ,  $T$ , and  $S'$  obtain VEVs or after  $U(1)'$  gauge symmetry breaking,  $(X D_i^c, X D_i)$  and  $(X L_i^c, X L_i)$  will become vector-like particles from the  $y_{ij}^{SD} X D_i^c X D_j S$  and  $y_{ij}^{SL} X L_i^c X L_j S$  terms,  $(D_i^c, X D_i)$  and  $(X L_i^c, L_i)$  will obtain vector-like masses from the  $y_{ij}^{TD} D_i^c X D_j T$  and  $y_{ij}^{TL} X L_i^c L_j T$  terms, and  $(X Q_k, \overline{X Q_k})$  will obtain vector-like masses from the  $y_{kl}^{XQ} S' \overline{X Q_k} X Q_l$  terms. After diagonalizing their mass matrices, we obtain the mixings between  $X D_i^c$  and  $D_i^c$ , and the mixings between  $X L_i$  and  $L_i$ . The discussion of the Higgs potential for electroweak symmetry breaking is similar to the Type II two Higgs doublet model, so we will not repeat it here. In addition, the third-generation quark masses are obtained directly from  $y_{33}^U Q_3 U_3^c H_u$  and  $y_{33}^D Q_3 D_3^c H_d$  terms, while the first two-generation quark masses are obtained by integrating out the vector-like particles  $(X Q_k, \overline{X Q_k})$  after  $U(1)'$  gauge symmetry breaking. Thus, we can explain why the first two-generation quarks are lighter than the third-generation in our model.

At low energy, the relevant degrees of freedom are SM particles,  $Z'$ , and DM  $\chi$ . The interactions can be expressed as

$$-\mathcal{L} = \sum_q g_u \bar{u} \gamma^\mu u Z'_\mu + g_{uA} \bar{u} \gamma^\mu \gamma^5 u Z'_\mu + g_d \bar{d} \gamma^\mu d Z'_\mu + g_{dA} \bar{d} \gamma^\mu \gamma^5 d Z'_\mu + g_\chi \bar{\chi} \gamma^\mu \chi Z'_\mu. \quad (9)$$

The ratio of different  $U(1)'$  couplings are determined by its  $U(1)'$  charge tabulated in Table II. Since our model is isospin-violated,  $u$  and  $d$  quarks couple different with  $Z'$ . After a brief

combination, we get

$$g_u : g_d : g_\chi : g_{dA} = 18 : -16 : -27 : -34, \quad g_{uA} = 0. \quad (10)$$

For example, if we set  $g_u = 0.1$ , then  $g_d = -0.0889$ ,  $g_\chi = -0.15$ ,  $g_{uA} = 0$ ,  $g_{dA} = -0.1889$ . Particularly, we do not have axial vector terms for  $u$ -quark in our model.

### III. CONSTRAINTS FROM DARK MATTER EXPERIMENTS

Generally, DM direct detection experiments assume DM couples the same to proton and neutron, and then report their limits for cross sections per nucleon. In the more general framework of IVDM, the cross sections per nucleon  $\sigma_N^Z$  is defined as

$$\sigma_N^Z = \sigma_p \frac{\sum_i \eta_i \mu_{A_i}^2 [Z + (A_i - Z) f_n/f_p]^2}{\sum_i \eta_i \mu_{A_i}^2 A_i^2} \equiv \frac{\sigma_p}{F_Z}, \quad (11)$$

where  $A_i$  refers to different isotopes and  $\eta_i$  is corresponding fractional number abundance. If  $\tilde{\sigma}$  is the limit reported by an experiment, then  $F_Z \tilde{\sigma}$  is the limit for IVDM. It is obvious that the DM elastic scattering off nucleus will have coherent effect between  $\sigma_p$  and  $\sigma_n$ , which can leads to a strongly destructive effect with particular  $f_n/f_p$ .

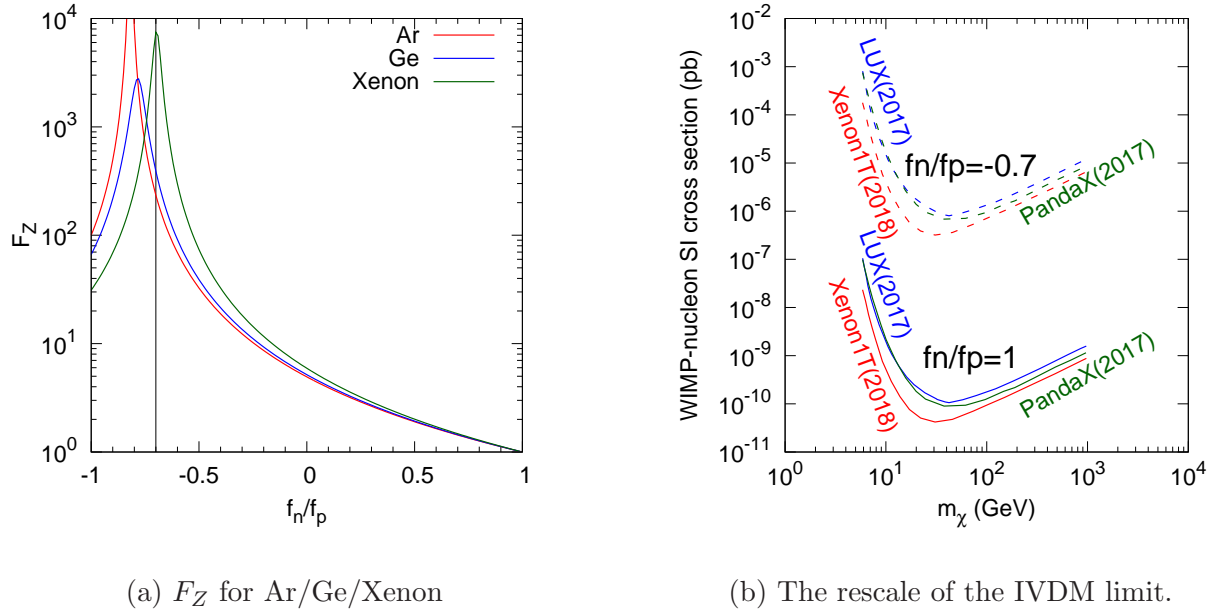


FIG. 1: The scaling factor  $F_Z$  for three different materials (left) and the rescaled limits of three Xenon based experiment (right), e.g., PandaX-II (2017) [9], LUX (2017) [10], and Xenon1T (2018) [11].

Previously, the IVDM with new experimental data has been studied in Ref. [38]. Here we update some experiment results and apply this bounds to our model. Shown in the left

panel of Fig. 1 are  $F_Z$  for three kinds of materials with isotopy effects taken into account. For the case of Xenon,  $F_Z$  get its maximum at  $f_n/f_p = -0.7$ . In the right panel of Fig. 1 we present the rescaled limits for three kinds of direct detection experiments. It is obvious that constraints of these Xenon based experiments could be relaxed by a factor of about  $10^{-4}$ .

It is well-known that for scalar and vector interaction, direct detection experiments have stronger capability to detect heavy DM with masses larger than 10 GeV, while collider searches have better sensitivity for small DM [39–42]. This conclusion would change dramatically once the isospin-violating effects are taken into account. In Figs. 2 and 3 we show the limits from direct detection experiment and indirect detection experiments. It is obvious that near the region of  $m_\chi \sim \frac{1}{2}m_{Z'}$ , the line of the correct DM relic density varies sharply due to resonant enhancement. Aside from the resonance region, DM direct detection experiments have better sensitivities than DM indirect detection experiments; while the latter give the best sensitivity around  $m_\chi \sim \frac{1}{2}m_{Z'}$ . In Figs. 2 and 3, we also demonstrate the region satisfying the observed relic density, which roughly trace the sensitivities of indirect detection experiment due to the  $s$ -wave annihilation nature of DM, as shown in the Appendix A.

#### IV. CONSTRAINTS FROM FUTURE COLLIDER

Another powerful methods to explore the nature of DM is collider search. In our model DM interacts directly with quarks, and can be copiously produced at hadron colliders such as the LHC and proposed LHC-hh [46] and SppC [47]. Once DM are produced, they will escape the detectors undetected, so another additional radiation is needed to trace these events. In this section we study the sensitivities of future colliders for this model, and compare them with those obtained from DM direct and indirect experiments. The techniques of collider research closely follow Ref. [42].

In this study, we focus on the monojet signal process  $pp \rightarrow Z'^{(*)} \rightarrow \chi\bar{\chi} + \text{jets}$ . The main backgrounds are  $Z(\rightarrow \bar{\nu}\nu) + \text{jets}$  and  $W(\rightarrow l\nu) + \text{jets}$ . Background and signal events at the parton level are generated with **MadGraph 5** [48] and then we use **PYTHIA 8** [49] to do parton shower and hadronization. MLM matching scheme are chose to avoid events double counting from matrix calculation and parton shower. We adopt **Delphes 3** [50] to perform fast detector simulation. Jets are reconstructed with anti- $K_T$  algorithm with a distance parameter  $R = 0.4$ . The future colliders would be constructed with higher resolution, so the results here are conservative and expected to be improved.

To improve the statistical significance, several cuts are implemented on both signal and background events. There must be at least two energetic jet in the final states. The leading jet  $j_1$  is required to have  $|\eta(j_1)| < 2.4$  and  $p_T(j_1) > 1.6/1.8/2.6$  TeV for  $\sqrt{s} = 33/50/100$  TeV. Events with more than two jets with  $p_T > 100$  GeV and  $|\eta| < 4$  are rejected. The DM

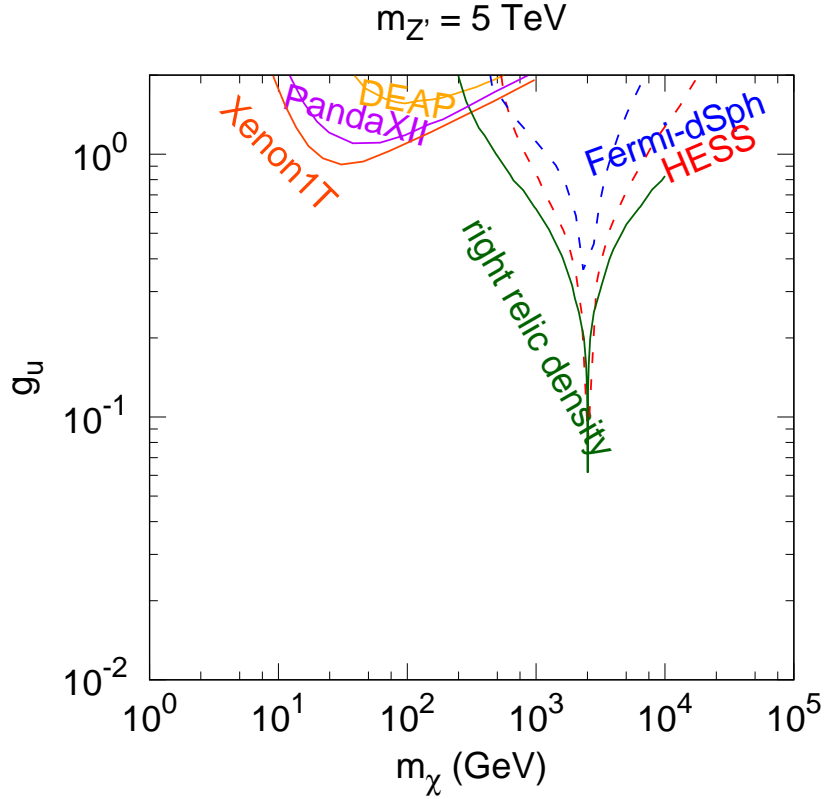


FIG. 2: Estimated 90% C.L. limits in  $m_\chi - g_u$  plane for direct detection experiments and indirect detection experiments. The solid orange, purple, and yellow lines correspond to PandaX-II (2017) [9], Xenon1T (2018) [11], DEAP3600 (2017) [43] experiments, respectively. The dashed blue and red lines correspond to Fermi-dSph (6-year) [44] and HESS (254h) [45], respectively. The dark-green line indicates the parameter space with the observed dark matter relic density.

production process may involve more than one jet from initial state radiation. In order to keep more signal events, a second jet( $j_2$ ) is allowed if it satisfies the condition  $\Delta\phi(j_1, j_2) < 2.5$ . The cut on  $\Delta\phi(j_1, j_2)$  is necessary to suppress the QCD multijet background, where large fake  $\cancel{E}_T$  may come from inefficient measurement of one of the jets. Furthermore, in order to reduce other backgrounds, such as  $W(\rightarrow lv) + \text{jets}$ ,  $Z(\rightarrow l^+l^-) + \text{jets}$ , and  $t\bar{t} + \text{jets}$  with leptonic top decays, the events containing isolated electrons, muons, taus, or photons with  $p_T > 20$  GeV and  $|\eta| < 2.5$  are discarded. We then count the events and present the exclusion limits at 95% C.L. in Fig. 4.

It is obvious from Fig. 4 that the sensitivity of collider strongly depends on whether  $Z'$  is on shell or not. When  $m_\chi < \frac{1}{2}m'_{Z'}$ ,  $Z'$  is on shell produced and the cross section is resonantly

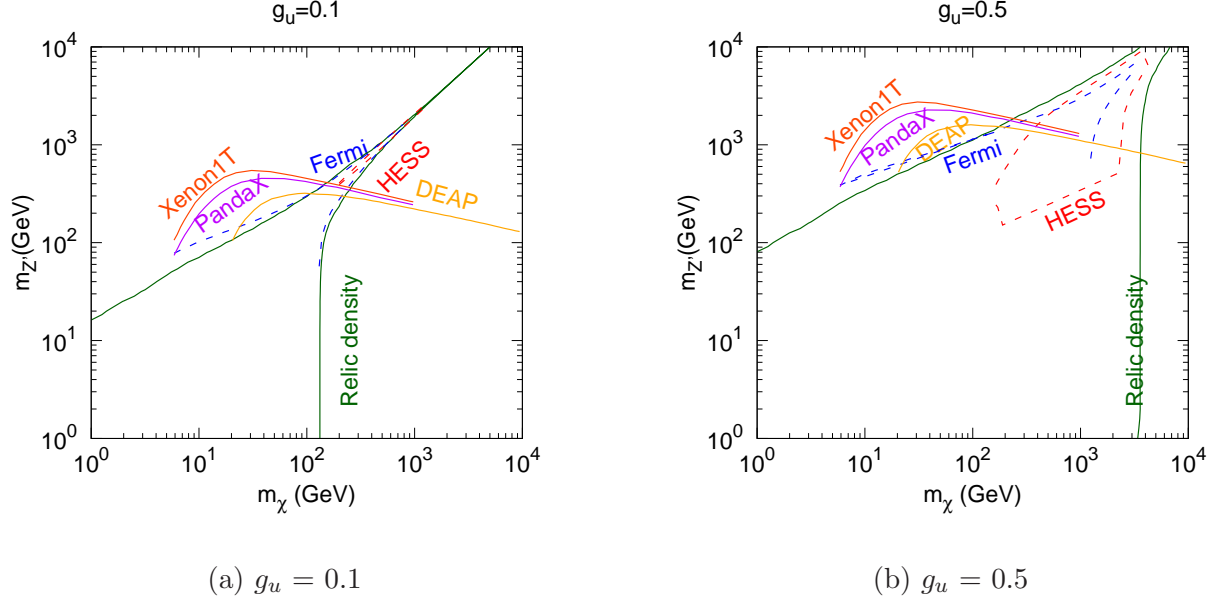


FIG. 3: The estimated 90% C.L. limits in  $m_\chi - m_{Z'}$  plane with the meaning of lines are the same in Fig. 2 .

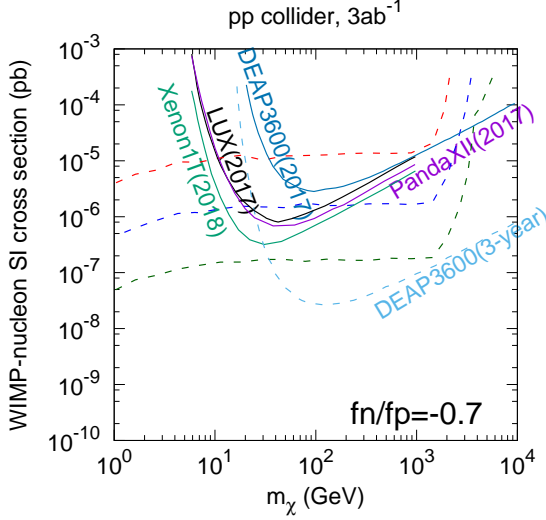
enhanced. In this case the DM production cross sections and collider sensitivities are almost independent of its mass. When  $m_\chi > \frac{1}{2}m'_{Z'}$ ,  $Z'$  is off shell produced, the DM production cross section is proportional to  $[g_q g_\chi / (Q^2 - m_{Z'}^2)]^2$  ( $Q^2$  is the typical momentum transfer to the DM pair) and is suppressed by  $1/Q^2$ . Particularly, for the case  $m_{Z'}^2 \ll Q^2$ , the DM cross section is proportional to  $[g_q g_\chi / Q^2]^2$  and is irrelevant to  $m_{Z'}$ , which is demonstrated in the left panel of Fig. 4 as that the solid and the dashed lines for the same color appear to close each other with the increase of  $m_\chi$ .

Compared to direct and indirect detections, the collider search would have stronger capability for the region  $m_\chi < \frac{1}{2}m'_{Z'}$ . Direct detection will be sensitive for  $m_\chi > 10$  GeV, while indirect detection will be sensitive for  $m_\chi > 100$  GeV, they could probe different mass regions and are complementary to each other.

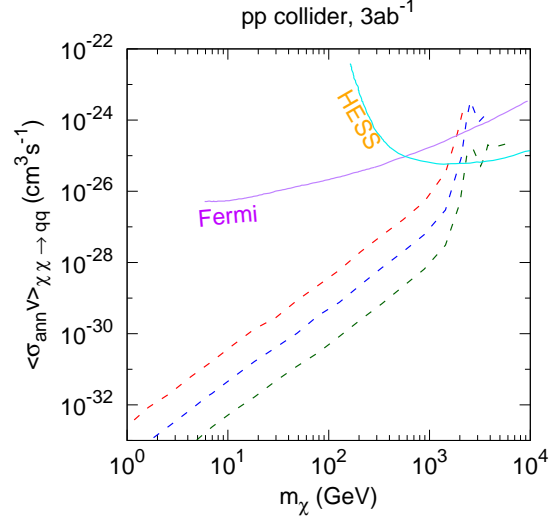
## V. CONCLUSIONS

We constructed a  $U(1)'$  model inspired by  $E_6$  which has the isospin-violating dark matter. After a few steps of gauge symmetry breaking, the unbroken gauge symmetry at TeV scale is  $SU(3)_C \times SU(2)_L \times U(1)_Y \times U(1)'$ . For the purpose of phenomenological study, we introduced some new particles to this model. Especially, due to the residual  $Z_2$  symmetry, an SM singlet fermion  $\chi$  with  $U(1)'$  charge  $-\mathbf{27}/\mathbf{2}$  is absolutely stable and then a DM candidate.

By choosing a proper linear combination of two extra  $U(1)$  gauge symmetries in  $E_6$ , we



(a) Direct detection vs future collider



(b) Indirect detection vs future collider

FIG. 4: The estimated limits for different detection methods. The red, blue, and dark-green lines correspond to future colliders with energy at  $\sqrt{s} = 33, 50$ , and  $100$  TeV, respectively. The dashed lines correspond to the benchmark choice with  $m_{Z'}$  equals to  $5$  TeV.

naturally obtained the ratio  $f_n/f_p = -0.7$  so as to maximally relax the constraints from the Xenon based direct detection experiments. Compared to isospin-conservation case, the constraints from the Xenon based experiments are relaxed by a factor of about  $\mathcal{O}(10^4)$ . We studied the sensitivities of dark matter direct and indirect detection experiments, and found the parameter spaces that have the observed relic density. For  $m_\chi \sim \frac{1}{2}m_{Z'}$ , the constraints from indirect detection experiments are enhanced due to resonance effects.

We then studied the sensitivities of the future colliders with center mass energy  $\sqrt{s} = 33/50/100$  TeV. The sensitivities of the collider searches are highly dependent on whether  $Z'$  is on-shell or not. Moreover, we compared the different detection methods, and showed that the future colliders will provide the much better searches in our model, especially for the region  $m_\chi < \frac{1}{2}m'_{Z'}$ .

## ACKNOWLEDGMENTS

The research of TL was supported by the Projects 11847612 and 11875062 supported by the National Natural Science Foundation of China, and by the Key Research Program of Frontier Science, CAS. QFX is supported by the China Postdoctoral Science Foundation under Grant No. 8206300015. And QSY and XHZ is supported by the Natural Science

Foundation of China under the grant No. 11475180 and No. 11875260.

## Appendix A: DM annihilation cross sections and relic density

In our IVDM model, DM annihilates into quarks to realize observed relic density, and the annihilation cross sections are

$$\begin{aligned}\sigma_{ann} = \sum_q & \frac{\beta_q c_q g_\chi^2}{12\pi\beta_\chi((s - m_{Z'}^2)^2 + m_{Z'}^2\Gamma_{Z'}^2)} \left( (g_{qV}^2(s + 2(m_q^2 + m_\chi^2) + 4\frac{m_q^2 m_\chi^2}{s}) \right. \\ & + g_{qA}^2(s + 4(m_q^2 + m_\chi^2) + 28\frac{m_q^2 m_\chi^2}{s} - 24\frac{m_q^2 m_\chi^2}{m_{Z'}^2} + 12\frac{s m_q^2 m_\chi^2}{m_{Z'}^4}) \\ & \left. + 2g_{qV}g_{qA}(s - (m_q^2 + m_\chi^2) - 8\frac{m_q^2 m_\chi^2}{s}) \right),\end{aligned}\quad (\text{A1})$$

where  $s$  is the squared center-of-mass energy of a DM particle pair and color factor  $c_q = 3$ .

$$\beta_f = \sqrt{1 - \frac{4m_f^2}{m_{Z'}^2}} \quad (f = q \text{ and } \chi).$$

The width of  $Z'$  can be expressed as

$$\Gamma_{Z'} = \Gamma(Z' \rightarrow \chi\bar{\chi}) + \sum_q c_q \Gamma(Z' \rightarrow q\bar{q}), \quad (\text{A2})$$

with

$$\Gamma(Z' \rightarrow q\bar{q}) = \frac{m_{Z'}}{12\pi} (g_{qA}^2 \xi_q (1 + \frac{2m_q^2}{m_{Z'}^2}) + g_{qV}^2 \xi_q^3), \quad (\text{A3})$$

$$\Gamma(Z' \rightarrow \chi\bar{\chi}) = \frac{m_{Z'}}{12\pi} g_\chi^2 (\xi_\chi (1 + \frac{2m_\chi^2}{m_{Z'}^2}) + \xi_\chi^3). \quad (\text{A4})$$

The particle explanation of  $Z'$  is  $\Gamma_{Z'} < m_{Z'}$ , which in turn roughly require  $g_u < 0.89$ .

In order to study DM relic density and indirect detection signals, we need to calculate the thermally averaged annihilation cross section  $\langle \sigma_{ann} v_M \rangle$ , where  $v_M \equiv \frac{\sqrt{(p_1 \cdot p_2)^2 - m_1^2 m_2^2}}{E_1 E_2}$  is the Moller velocity. However, instead of calculating  $\langle \sigma_{ann} v_M \rangle$  directly, it is more convenient to calculate  $\langle \sigma_{ann} v_{rel} \rangle$  in the laboratory frame, which means one of the initial particles is at rest, and get the same result. Here  $v_{rel}$  is the relative velocity between them.

In the laboratory frame, when DM is non-relativistic,  $s$  can be expanded as  $4m_\chi^2 + m_\chi^2 v^2 + \frac{3}{4}m_\chi^2 v^4 + \mathcal{O}(v^6)$ , with  $v \equiv v_{rel} = \beta_\chi (1 - \frac{2m_\chi^2}{s})^{-1}$ . Plugging this expression into Eq. (A1),

one can expand  $\sigma_{ann}v$  as  $a + bv^2 + \mathcal{O}(v^4)$  with coefficients  $a$  and  $b$  given by

$$a = \sum_q \frac{c_q g_\chi^2 \sqrt{1 - \frac{m_q^2}{m_\chi^2}} (2g_A g_V (m_\chi^2 - m_q^2) m_{Z'}^4 + g_A^2 m_q^2 (m_{Z'}^2 - 4m_\chi^2)^2 + g_V^2 (m_q^2 + 2m_\chi^2) m_{Z'}^4)}{2\pi m_{Z'}^4 ((m_{Z'}^2 - 4m_\chi^2)^2 + m_{Z'}^2 \Gamma_{Z'}^2)} \quad (\text{A5})$$

$$b = \sum_q \frac{v^2 c_q g_\chi^2}{48\pi m_\chi^2 \sqrt{1 - \frac{m_q^2}{m_\chi^2}} m_{Z'}^4 ((m_{Z'}^2 - 4m_\chi^2)^2 + m_{Z'}^2 \Gamma_{Z'}^2)^2} \times$$

$$\begin{aligned} & (-2g_A g_V (m_q^2 - m_\chi^2) m_{Z'}^4 (m_q^2 (400m_\chi^4 + 13m_{Z'}^2 (m_{Z'}^2 + \Gamma_{Z'}^2) - 152m_\chi^2 m_{Z'}^2) \\ & + 2m_\chi^2 (-80m_\chi^4 + m_{Z'}^2 \Gamma_{Z'}^2 + 16m_\chi^2 m_{Z'}^2 + m_{Z'}^4)) + g_A^2 (m_q^4 (3840m_\chi^8 + 16m_\chi^4 (3m_{Z'}^2 \Gamma_{Z'}^2 + 98m_{Z'}^4) \\ & - 8m_\chi^2 (9m_{Z'}^4 \Gamma_{Z'}^2 + 38m_{Z'}^6) + 23m_{Z'}^6 (m_{Z'}^2 + \Gamma_{Z'}^2) - 3840m_\chi^6 m_{Z'}^2) \\ & - 4m_q^2 m_\chi^2 (768m_\chi^8 - 4m_\chi^2 (3m_{Z'}^4 \Gamma_{Z'}^2 + 20m_{Z'}^6) + 7m_{Z'}^6 (m_{Z'}^2 + \Gamma_{Z'}^2) - 768m_\chi^6 m_{Z'}^2 + 352m_\chi^4 m_{Z'}^4) \\ & + 8m_\chi^4 m_{Z'}^4 (16m_\chi^4 + m_{Z'}^2 \Gamma_{Z'}^2 - 8m_\chi^2 m_{Z'}^2 + m_{Z'}^4)) \\ & + g_V^2 m_{Z'}^4 (m_q^4 (368m_\chi^4 + 11m_{Z'}^2 (m_{Z'}^2 + \Gamma_{Z'}^2) - 136m_\chi^2 m_{Z'}^2) \\ & + 2m_q^2 m_\chi^2 (112m_\chi^4 + m_{Z'}^2 \Gamma_{Z'}^2 - 32m_\chi^2 m_{Z'}^2 + m_{Z'}^4) \\ & - 4m_\chi^4 (112m_\chi^4 + m_{Z'}^2 \Gamma_{Z'}^2 - 32m_\chi^2 m_{Z'}^2 + m_{Z'}^4))) \end{aligned} \quad (\text{A6})$$

To get relic density, we can use an approximate function instead of solving the Boltzmann equation numerically

$$\Omega_\chi h^2 = 2 \times 1.04 \times 10^9 \text{GeV}^{-1} \left( \frac{T_0}{2.725 \text{ K}} \right)^3 \frac{x_f}{M_{pl} \sqrt{g_*(x_f)} (a + \frac{3b}{x_f})} \quad (\text{A7})$$

where  $x_f \equiv \frac{m_\chi}{T_f} \sim \mathcal{O}(10)$ ,  $T_f$  is the DM freeze-out temperature,  $T_0 = 2.725 \pm 0.002 \text{ K}$  is the present CMB temperature, and  $g_*(x_f)$  is the effective relativistic degrees of freedom at the freeze-out epoch.

- 
- [1] **DAMA** Collaboration, R. Bernabei et al., *Search for WIMP annual modulation signature: Results from DAMA / NaI-3 and DAMA / NaI-4 and the global combined analysis*, Phys. Lett. B **480** (2000) 23–31.
  - [2] **DAMA** Collaboration, R. Bernabei et al., *First results from DAMA/LIBRA and the combined results with DAMA/NaI*, Eur. Phys. J. **C56** (2008) 333–355, [[arXiv:0804.2741](#)].
  - [3] **DAMA, LIBRA** Collaboration, R. Bernabei et al., *New results from DAMA/LIBRA*, Eur. Phys. J. **C67** (2010) 39–49, [[arXiv:1002.1028](#)].
  - [4] R. Bernabei et al., *Final model independent result of DAMA/LIBRA-phase1*, Eur. Phys. J. **C73** (2013) 2648, [[arXiv:1308.5109](#)].
  - [5] R. Bernabei et al., *First Model Independent Results from DAMA/LIBRA Phase2*, Universe **4** (2018), no. 11 116, [[arXiv:1805.10486](#)]. [[Nucl. Phys. Atom. Energy](#) 19, no. 4, 307 (2018)].

- [6] **CoGeNT** Collaboration, C. E. Aalseth et al., *Results from a Search for Light-Mass Dark Matter with a P-type Point Contact Germanium Detector*, Phys. Rev. Lett. **106** (2011) 131301, [[arXiv:1002.4703](#)].
- [7] C. E. Aalseth et al., *Search for an Annual Modulation in a P-type Point Contact Germanium Dark Matter Detector*, Phys. Rev. Lett. **107** (2011) 141301, [[arXiv:1106.0650](#)].
- [8] G. Angloher et al., *Results from 730 kg days of the CRESST-II Dark Matter Search*, Eur. Phys. J. **C72** (2012) 1971, [[arXiv:1109.0702](#)].
- [9] **PandaX-II** Collaboration, X. Cui et al., *Dark Matter Results From 54-Ton-Day Exposure of PandaX-II Experiment*, Phys. Rev. Lett. **119** (2017), no. 18 181302, [[arXiv:1708.06917](#)].
- [10] **LUX** Collaboration, D. S. Akerib et al., *Results from a search for dark matter in the complete LUX exposure*, Phys. Rev. Lett. **118** (2017), no. 2 021303, [[arXiv:1608.07648](#)].
- [11] **XENON** Collaboration, E. Aprile et al., *Dark Matter Search Results from a One Ton-Year Exposure of XENON1T*, Phys. Rev. Lett. **121** (2018), no. 11 111302, [[arXiv:1805.12562](#)].
- [12] J. L. Feng, J. Kumar, D. Marfatia, and D. Sanford, *Isospin-Violating Dark Matter*, Phys. Lett. **B703** (2011) 124–127, [[arXiv:1102.4331](#)].
- [13] G. Adhikari et al., *An experiment to search for dark-matter interactions using sodium iodide detectors*, Nature **564** (2018), no. 7734 83–86. [Erratum: Nature566,no.7742,E2(2019)].
- [14] S. Kang, S. Scopel, G. Tomar, and J.-H. Yoon, *Proton-philic spin-dependent inelastic dark matter as a viable explanation of DAMA/LIBRA-phase2*, Phys. Rev. **D99** (2019), no. 2 023017, [[arXiv:1810.09674](#)].
- [15] K. Hamaguchi, S. P. Liew, T. Moroi, and Y. Yamamoto, *Isospin-Violating Dark Matter with Colored Mediators*, JHEP **05** (2014) 086, [[arXiv:1403.0324](#)].
- [16] A. Drozd, B. Grzadkowski, J. F. Gunion, and Y. Jiang, *Isospin-violating dark-matter-nucleon scattering via two-Higgs-doublet-model portals*, JCAP **1610** (2016), no. 10 040, [[arXiv:1510.07053](#)].
- [17] M. T. Frandsen, F. Kahlhoefer, S. Sarkar, and K. Schmidt-Hoberg, *Direct detection of dark matter in models with a light  $Z'$* , JHEP **09** (2011) 128, [[arXiv:1107.2118](#)].
- [18] G. Blanger, A. Goudelis, J.-C. Park, and A. Pukhov, *Isospin-violating dark matter from a double portal*, JCAP **1402** (2014) 020, [[arXiv:1311.0022](#)].
- [19] V. M. Lozano, M. Peir, and P. Soler, *Isospin violating dark matter in Stckelberg portal scenarios*, JHEP **04** (2015) 175, [[arXiv:1503.01780](#)].
- [20] Z. Kang, T. Li, T. Liu, C. Tong, and J. M. Yang, *Light Dark Matter from the  $U(1)_X$  Sector in the NMSSM with Gauge Mediation*, JCAP **1101** (2011) 028, [[arXiv:1008.5243](#)].
- [21] X. Gao, Z. Kang, and T. Li, *Origins of the Isospin Violation of Dark Matter Interactions*, JCAP **1301** (2013) 021, [[arXiv:1107.3529](#)].

- [22] A. Crivellin, M. Hoferichter, M. Procura, and L. C. Tunstall, *Light stops, blind spots, and isospin violation in the MSSM*, JHEP **07** (2015) 129, [[arXiv:1503.03478](#)].
- [23] F. Gursev, P. Ramond, and P. Sikivie, *A Universal Gauge Theory Model Based on  $E_6$* , Phys. Lett. **60B** (1976) 177–180.
- [24] Y. Achiman and B. Stech, *Quark Lepton Symmetry and Mass Scales in an  $E_6$  Unified Gauge Model*, Phys. Lett. **77B** (1978) 389–393.
- [25] Q. Shafi,  *$E(6)$  as a Unifying Gauge Symmetry*, Phys. Lett. **79B** (1978) 301–303.
- [26] P. Ramond, *The Family Group in Grand Unified Theories*, in International Symposium on Fundamentals of Quantum Theory and Quantum Field Theory Palm Coast, FL pp. 265–280, 1979. [hep-ph/9809459](#).
- [27] P. Langacker, *The Physics of Heavy  $Z'$  Gauge Bosons*, Rev. Mod. Phys. **81** (2009) 1199–1228, [[arXiv:0801.1345](#)].
- [28] J. Erler, *Chiral models of weak scale supersymmetry*, Nucl. Phys. **B586** (2000) 73–91, [[hep-ph/0006051](#)].
- [29] P. Langacker and J. Wang,  *$U(1)$ -prime symmetry breaking in supersymmetric  $E(6)$  models*, Phys. Rev. **D58** (1998) 115010, [[hep-ph/9804428](#)].
- [30] J. Erler, P. Langacker, and T.-j. Li, *The  $Z - Z'$  mass hierarchy in a supersymmetric model with a secluded  $U(1)$  -prime breaking sector*, Phys. Rev. **D66** (2002) 015002, [[hep-ph/0205001](#)].
- [31] J. Kang, P. Langacker, T.-j. Li, and T. Liu, *Electroweak baryogenesis in a supersymmetric  $U(1)$ -prime model*, Phys. Rev. Lett. **94** (2005) 061801, [[hep-ph/0402086](#)].
- [32] J.-h. Kang, P. Langacker, and T.-j. Li, *Neutrino masses in supersymmetric  $SU(3)(C) \times SU(2)(L) \times U(1)(Y) \times U(1)$ -prime models*, Phys. Rev. **D71** (2005) 015012, [[hep-ph/0411404](#)].
- [33] J. Kang, P. Langacker, T. Li, and T. Liu, *Electroweak Baryogenesis, CDM and Anomaly-free Supersymmetric  $U(1)'$  Models*, JHEP **04** (2011) 097, [[arXiv:0911.2939](#)].
- [34] R. Slansky, *Group Theory for Unified Model Building*, Phys. Rept. **79** (1981) 1–128.
- [35] J. L. Hewett and T. G. Rizzo, *Low-Energy Phenomenology of Superstring Inspired  $E(6)$  Models*, Phys. Rept. **183** (1989) 193.
- [36] S. F. King, S. Moretti, and R. Nevzorov, *Theory and phenomenology of an exceptional supersymmetric standard model*, Phys. Rev. **D73** (2006) 035009, [[hep-ph/0510419](#)].
- [37] K. S. Babu, B. Bajc, and V. Susi, *A minimal supersymmetric  $E_6$  unified theory*, JHEP **05** (2015) 108, [[arXiv:1504.00904](#)].
- [38] C. E. Yaguna, *Isospin-violating dark matter in the light of recent data*, Phys. Rev. **D95** (2017), no. 5 055015, [[arXiv:1610.08683](#)].

- [39] A. Alves, S. Profumo, and F. S. Queiroz, *The dark  $Z'$  portal: direct, indirect and collider searches*, JHEP **04** (2014) 063, [[arXiv:1312.5281](#)].
- [40] O. Buchmueller, M. J. Dolan, S. A. Malik, and C. McCabe, *Characterising dark matter searches at colliders and direct detection experiments: Vector mediators*, JHEP **01** (2015) 037, [[arXiv:1407.8257](#)].
- [41] J. Abdallah et al., *Simplified Models for Dark Matter and Missing Energy Searches at the LHC*, [arXiv:1409.2893](#).
- [42] Q.-F. Xiang, X.-J. Bi, P.-F. Yin, and Z.-H. Yu, *Searches for dark matter signals in simplified models at future hadron colliders*, Phys. Rev. **D91** (2015) 095020, [[arXiv:1503.02931](#)].
- [43] **DEAP-3600** Collaboration, P. A. Amaudruz et al., *First results from the DEAP-3600 dark matter search with argon at SNOLAB*, Phys. Rev. Lett. **121** (2018), no. 7 071801, [[arXiv:1707.08042](#)].
- [44] **Fermi-LAT** Collaboration, M. Ackermann et al., *The Fermi Galactic Center GeV Excess and Implications for Dark Matter*, Astrophys. J. **840** (2017), no. 1 43, [[arXiv:1704.03910](#)].
- [45] **H.E.S.S.** Collaboration, H. Abdallah et al., *Search for dark matter annihilations towards the inner Galactic halo from 10 years of observations with H.E.S.S.*, Phys. Rev. Lett. **117** (2016), no. 11 111301, [[arXiv:1607.08142](#)].
- [46] **FCC** Collaboration, A. Abada et al., *FCC-hh: The Hadron Collider*, Eur. Phys. J. ST **228** (2019), no. 4 755–1107.
- [47] M. Ahmad et al., *CEPC-SPPC Preliminary Conceptual Design Report. 1. Physics and Detector*, .
- [48] J. Alwall, R. Frederix, S. Frixione, V. Hirschi, F. Maltoni, O. Mattelaer, H. S. Shao, T. Stelzer, P. Torrielli, and M. Zaro, *The automated computation of tree-level and next-to-leading order differential cross sections, and their matching to parton shower simulations*, JHEP **07** (2014) 079, [[arXiv:1405.0301](#)].
- [49] T. Sjostrand, S. Mrenna, and P. Z. Skands, *A Brief Introduction to PYTHIA 8.1*, Comput. Phys. Commun. **178** (2008) 852–867, [[arXiv:0710.3820](#)].
- [50] **DELPHES 3** Collaboration, J. de Favereau, C. Delaere, P. Demin, A. Giammanco, V. Lematre, A. Mertens, and M. Selvaggi, *DELPHES 3, A modular framework for fast simulation of a generic collider experiment*, JHEP **02** (2014) 057, [[arXiv:1307.6346](#)].